Renewable Energy 86 (2016) 1256–1264

Contents lists available at ScienceDirect

Renewable Energy

journal homepage: www.elsevier.com/locate/renene

Thermal infrared imaging of geothermal environments and by an unmanned aerial vehicle (UAV): A case study of the Wairakei – Tauhara geothermal field, Taupo, New Zealand

Abdul Nishar [a, *], Steve Richards [b], Dan Breen [a], John Robertson [a], Barbara Breen [a, **]

[a] School of Applied Sciences, AUT University, Auckland, New Zealand
[b] Poseidon Consulting Ltd, Taupo, New Zealand

ARTICLE INFO

Article history:
Received 24 May 2015
Received in revised form
24 August 2015
Accepted 20 September 2015

Keywords:
UAV
GIS
Remote sensing
Thermal infrared imaging
Geothermal
Aerial monitoring

ABSTRACT

Recent advances in unmanned aerial vehicles (UAVs) for civilian use make it possible to regularly monitor geothermal environments at spatial and temporal scales that would be difficult to achieve using conventional methods. Previous aerial monitoring of geothermal environments has been expensive and time consuming. This paper demonstrates the use of a small (<2 kg), cost effective quadcopter UAV to safely and accurately map physical and biological characteristics of these unique habitats. Thermal infrared imaging and photogrammetry are used to capture detailed information of geothermal surface features and surrounding vegetation within the Wairakei – Tauhara geothermal field near Taupo, New Zealand. The study highlights advanced techniques in sampling, processing and analysing UAV images and identifies some research challenges and limitations in the use of UAV platforms and sensors. The application of UAVs to describe and monitor geothermal features and other environments is a rapidly developing field in science and natural resource management. This project demonstrates the utility of UAV applications in geothermal science and the potential for their use in many other areas of research.

1. Introduction

Geothermal systems occur in regions of high subsurface heat flow related to hot rock located deeper in the earth's crust [26,84]. Geothermal heat trapped in fluid filled fractures and permeable rocks has been used for both domestic and commercial practises. In New Zealand, geothermal systems have been used for heating and cooking by Maori for centuries [6,101]. Geothermal energy has also been used for electricity generation with the first geothermal power plant commissioned in New Zealand at Wairakei in 1958 [23,98].

Around the world, geothermal energy accounts for a significant proportion of power production [33,64]. The Central North Island contains all but one of New Zealand's geothermal systems generating 10% of New Zealand's electricity supplies [9]. Geothermal energy is a cost effective, renewable source of energy with minimal carbon outputs unlike coal burning power stations. There is, therefore, worldwide interest in geothermal power and there are increasing efforts to explore and characterise geothermal resources [41].

Ref. [45] describes geothermal systems as convective water in the upper crust of the Earth transferring heat to the surface. A geothermal system is made up of three main elements: a heat source, a reservoir and a fluid that transfers the heat [25]. Elevated geothermal heat is usually transferred to the surface by the convection of ground water [44,78,80]. Heat may emerge at the surface as hot springs, fumaroles, mud pools, and geysers [42]. Geothermal systems may however lack obvious surface features and are referred to as surface blind geothermal systems. In these cases, impermeable layers limit the continuous flow of hot fluids and gases to the surface [40] and can be difficult to identify. But despite this, these blind features have the same level of significance as the surface features for geothermal resource assessment and utilisation.

It has been recognised since the 1970's that aerial thermal infrared surveys (TIR) can be used to monitor both known and blind geothermal systems [24,61]. While reflected data mainly providing spectral information on the surface characteristics of the landscape [65], thermal infrared data provides additional spectral information of both surface and subsurface conditions [19,85]. The aerial TIR surveying method is applicable wherever there is temperature difference in the environment [50]. TIR imagery has been demonstrated to supply information which was previously a missing element in many fields [93]. The Wairakei and Tauhara geothermal fields were

* Corresponding author.
** Corresponding author.
E-mail addresses: abdul_nishar@xtra.co.nz (A. Nishar), barbara.breen@aut.ac.nz (B. Breen).

http://dx.doi.org/10.1016/j.renene.2015.09.042
0960-1481/

the first to be surveyed by TIR in New Zealand [24]. Thermal imaging has since become a fundamental tool for geothermal monitoring [71,72], with district councils regulating the geothermal fields requiring consent holders to conduct TIR surveys as part of their own environmental monitoring programs. It is beneficial to collect TIR data over the area of interest at a regular interval regularly or repeatedly [5,50] to allow geothermal developers and resource managers to respond to changes in geothermal systems more proactively rather than after adverse changes have occurred [62]. The conventional practice of TIR aerial data collection is using manned aircraft [24,71,72], which is expansive due to the cost of the commissioned flight and the number of technical resources involved; influencing the frequency of the survey. However, this situation is unlikely to improve unless the costs associated with TIR data collection become more affordable.

UAVs are also sometimes referred to as UAS (unmanned airborne systems) or even RPAS (remotely piloted aerial systems), can be consideration an alternative. A UAV platform is capable of carrying different measuring devices [100] and can be controlled manually by a trained person on the ground or flown autonomously according to a pre-programmed flight plan. UAVs were initially developed for military missions too difficult for manned aircraft [99]. There are a variety of UAVs available that are employed for various civil, industrial and agricultural research and management [59,95,111]. Their size varies with the required payload, range and purpose [3,4,18,51,73], from as small as a bird to as large as a human piloted aeroplane [29].

In addition to their advantages in hazardous conditions, UAVs have other advantages including low cost, smaller dimensions, flexibility and the ability to reliably fly at low altitudes and around obstacles [70,74]. UAVs provide a tool that complements other remote sensing technologies [8] and are better suited to regional scale studies [77]. Processing and analysis of UAV data has been assisted significantly through recent advances in geographical information systems (GIS), mosaicking and image recognition [66,102].

The purpose of this paper is to highlight the cost effective techniques for the collection of TIR imagery using an unmanned aerial vehicle (UAV) and an efficient workflow to process and analyse the data collected. Also, this paper aims to demonstrate the high quality of output using this new methodology. The main motivation for employing the UAV was to precisely map the geothermal heat signature of a geothermal feature found in the Wairakei – Tauhara geothermal field, Taupo, New Zealand. Overall, the aim was to take advantage of a convenient and economical solution for TIR data collection, as opposed to contracting a costly and time consuming manned mission.

2. Wairakei – Tauhara geothermal system

The Taupo Volcanic Zone (TVZ) is an area of intense geothermal activity in the North Island of New Zealand [53,91]. It is an area approximately 30 km wide by 150 km long and contains 23 geothermal fields or systems [10]. The structure of the TVZ geothermal fields was examined by Ref. [109] who concluded that the majority were located at the margins of major volcanic craters. The TVZ contains all but one of New Zealand's geothermal systems [43]. The 23 geothermal systems identified within the TVZ [10] have different heat outputs [53] but once formed, are stable and long-lived [10].

Each geothermal field is typically 5–25 km^2 in area [10] and appear to be regularly spaced, with an average separation of about 15 km [68,110]. Based on geology [38], estimates the age of Wairakei–Tauhara geothermal field to be at least 0.5 million years old. The Wairakei–Tauhara geothermal field appears to have maintained activity during recent volcanism [90], and has the largest observed heat flows in the TVZ [53].

Due to its suitability for power generation, the TVZ has received previous attention by investors [16,54,108]. Since the TVZ has high heat flow [46], gives a figure of 2600 MWe heat flow in the 100 km^2 area within the TVZ. There are currently five fields within the TVZ used for geothermal electricity with a generation capacity of about 750 MWe.

Despite the challenging environments, the Wairakei–Tauhara geothermal field supports a unique ecosystem. The survival of life near such high temperatures, has inspired studies by many researchers [12–14,20,22] and has attracted a strong ecological interest [7,75,81] in the Wairakei–Tauhara geothermal field. The plants species that are found and grow in the geothermal fields are often rare and some are even endemic to this ecosystem [17,36].

As the Wairakei–Tauhara geothermal field covers such a wide area, the local council has divided the field into hot ground boundaries based on the surface manifestations. A section of a surface manifestation within the largest hot ground boundary was selected for this study. The site lies within a geothermal reservation area and is protected against any commercial developments. It is owned by the Tauhara Middle 15 Trust who have consented to this study being conducting on their land. Fig. 1, indicates the extent of the TVZ, the Wairakei – Tauhara geothermal field and the study area.

3. Materials and methods

3.1. Equipment

3.1.1. Platform

Geothermal areas present a unique environmental and geographic challenge. The UAV must be able to take-off and land in rugged terrain, stable, capable of carrying a high-resolution camera, withstand steam and wind, and remain light enough to be easily carried into the field by one person. All of the fixed-wing platforms were eliminated because of launch and recovery constraints of fixed-wing aircraft and the challenges faced by small fixed-wing aircraft in manoeuvring over and collecting high-resolution images and overlaps of small targets in moderate winds [47,106]. The category of platforms that seemed to meet all of our criteria was the small multi-rotor, battery-powered vertical take-off and landing vehicle. These aircraft are easy and safe to operate, can hover over the target area during photographic operations, and can take off and land almost anywhere [34]. We therefore selected Blade 350 QX2 Quadcopter.

A Blade 350 QX2 Quadcopter with a Spektrum DX5e DSMX 5-Channel transmitter (by Horizon Hobby, LLC) was used to fly over the study area. The UAV has GPS and compass functionality, weighs approximately 1 kg including the battery and camera, has an 8–12 min flight time and a controlled maximum height of up to 45 m in “smart” mode depending on the needs of the mission. The quadcopter has other flight modes for more experienced operators but for survey work smart mode is used exclusively. The quadcopter also has an autonomous return home functionality which can be engaged at any time or engages automatically if communication is lost. For this study, smart mode was used to reliably capture data with wind speeds of up to 20 km h^{-1}.

3.1.2. Camera and sensor

A Sony HDR-AS100V mounted below the quadcopter was used to capture colour (RGB) aerial images and a FLIR Tau 320 camera and sensor was used to capture thermal infrared videos. Table 1, lists the specifications for both devices. The Sony camera weighed 92 g, measured 24.2 mm × 46.5 mm × 81.5 mm and was enclosed in the supplied splash proof case. Geotagged images at 13.5 megapixel resolution were captured at 1 s capture intervals.

The FLIR unit used a FLIR Tau 320 sensor with a FLIR 25 mm lens

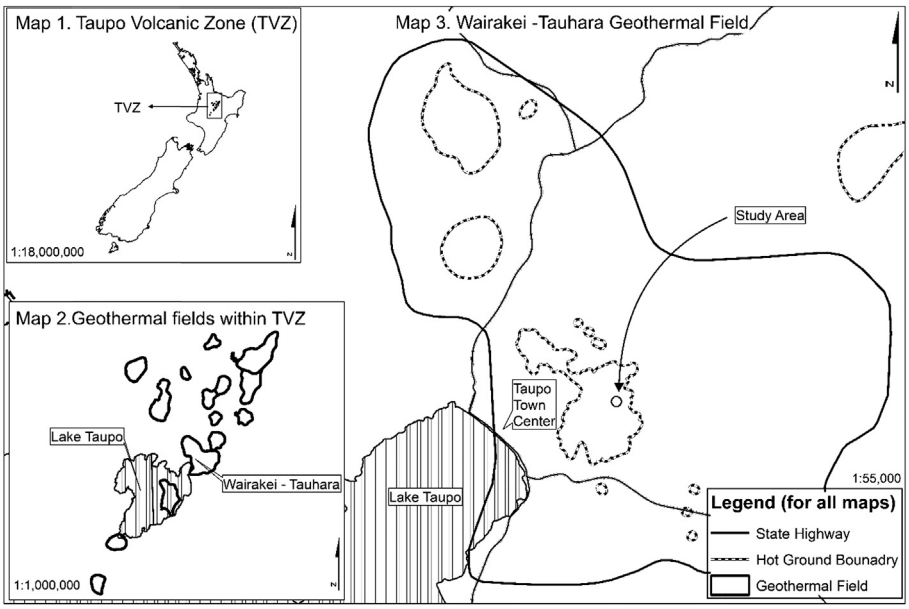

Fig. 1. Taupo Volcanic Zone – Geothermal fields. (Data source: Waikato Regional Council and Taupo District Council). Map 1 Location of TVZ in New Zealand. Map 2 geothermal fields in the TVZ. Map 3 The Wairakei – Tauhara geothermal field, the hot ground boundaries allocated by Taupo District Council and the study site.

Table 1
Camera and sensor specifications for the Sony HDR-AS100V and the FLIR's Tau 320).

Sony POV action cam (HDR-AS100V)	FLIR's Tau 320
Lens type: ZEISS tessar	Thermal imager: uncooled VOx microbolometer
Aperture: F2.8	FPA formats 324 × 256
Focal length: f = 15.3 mm (170°), f = 21.3 mm (120°)	Pixel size: 25-micron
Minimum focus distance: approx. 30 cm	Full frame rate: 30 Hz (NTSC); 25 Hz (PAL)
Focal distance: f = 2.5 mm	Exportable frame rates: 7.5 Hz (NTSC); 8.3 Hz (PAL)
CCD resolution: 13.5 megapixels	Input power: 4.0–6.0 VDC
Dimensions: 1.8 by 0.95 by 3.2 inches	Power dissipation: <1 W
Image stabilization: digital	Sensitivity: <50 mk f/1.0
Interface ports: micro USB	Time to image, FFC interval: <3.5 s, <0.5 s
LCD size: 1 inches	Size: 1.75" × 1.75" × 1.18″
Mic input jack: Yes	Operating temperature range: −40 °C to +80 °C
Sensor type: CMOS	Non-operating temperature range: −55 °C to +105 °C
Still image mode: JPEG	Tau lens resolution: 320 × 240
Video format: MPEG4-AVC/H.264	Tau lens FOV (H × V): 18° × 14°
Waterproof depth (Mfr. Rated):16.5 feet	Tau lens f/#:1.1
Video resolution:1080p	Tau lens weight: 135 g

Table 2
Description of the cloud computer used.

Cloud compter used:
Windows 8, server 2012, 64 bits 16 CPU 32 GB RAM, 10 GB HDD free space.

and Flashback 3 single recorder writing to a full size SD card. The unit was operated in its standard 8.3 fps PAL video mode. The whole unit was mounted in a custom made 2 mm birch ply and carbon fibre case covered with aluminium foil covering to shield the UAV from RF noise. Power for the unit was taken from one cell (4 V nominal) from the voltage balancing plug on the 3 cell 11.1 V lithium polymer flight battery. The Tau 320 is also equipped with a FLIR Tau Photon Replicator Board which communicates via a 30-pin SAMTEC connector and allows the use of voltage inputs between 6 and 27 V.

Power comes from one cell off the balance plug on the flight battery. FLIR Tau 320 is capable of detecting wavelengths in the range of 8–14 microns. The camera is light weight and has up to a 921600 Baud rate which allows quicker interaction with a computer or laptop [32,57]. and [97] have successfully used FLIR Tau 320 cameras to address their research needs. The video files need to be downloaded from the camera to be viewed, as the camera does not come with a built-in preview screen.

Both the cameras had a wide angle lens which were suitable to be mounted facing directly downward on a UVA to capture data over a reasonably flat study site [67]. The Sony HDR-AS100V being an action camera is shockproof as well as comes with a built-in image stabilization function [103] to reduce the effects of sudden movement and vibration. FLIR Tau 320 sensor is built to endure shock up to 200 g shock w/11 mSec [37], this provides sufficient tolerance to unforeseen movements while in air.

3.1.3. Image acquisition

In order to geo-reference UAV imagery in the absence of precise navigation data, Ground Control Points (GCP) are required. For optical images, natural GCPs are the norm. In contrast, in many cases it is not possible to find natural GCPs in thermal images which appear sufficiently crisp and can be located accurately thus we decided to use artificial GCPs. We used aluminium as the material for the GCPs. Five control points (30 cm paper plates covered with aluminium foil) were arranged within the study area. Aluminium sheets have a sharp boundary in a thermal image [83].

The 700 m^2 study area was flown separately with the colour camera and then later with the thermal infrared camera. Although the UAV is capable of flying in slight rain and windy condition, it was not done due to high risk to the sensors and aircrafts performance. Wind speed and rain forecast was checked on the metrological services website before all flights. Wind speeds up to 20 km/h were within the safe operation procedures. This standard was strictly followed due to the concerns that strong wind could hinder

the stability of the drone, affecting the image quality. Furthermore, strong winds made the landing in dusk light much more complicated and uncertain. To reduce the impact of solar radiation, flights were flown at dusk. While it is preferable to capture thermal infrared data at night, New Zealand Civil Aviation regulations (https://www.caa.govt.nz) do not permit the use of UAV's at night. Due to the time window and the level of overlap necessary, thermal data were captured over eight separate occasions.

To obtain high resolution thermal infrared images and sufficient overlapping images, the quadcopter was flown at a slow speed, at an altitude of 20 m repeatedly across the study site (Fig. 2) taking photographs every 1 s. In order to acquire images with sufficient overlap, the UAV was flown along both the long and short axes of the study area (Fig. 2a).

Geotagged colour aerial images were captured showing the GCPs to use for georeferencing. For the capture of colour images, two flight missions were carried out, between 11am and 2pm on each flight to minimise the influence of shadow on the imagery. Fig. 2 shows the flight path followed to collect colour aerial imagery. The same flying procedure was followed, only the flight time and overlap requirement differed between colour missions and thermal infrared missions.

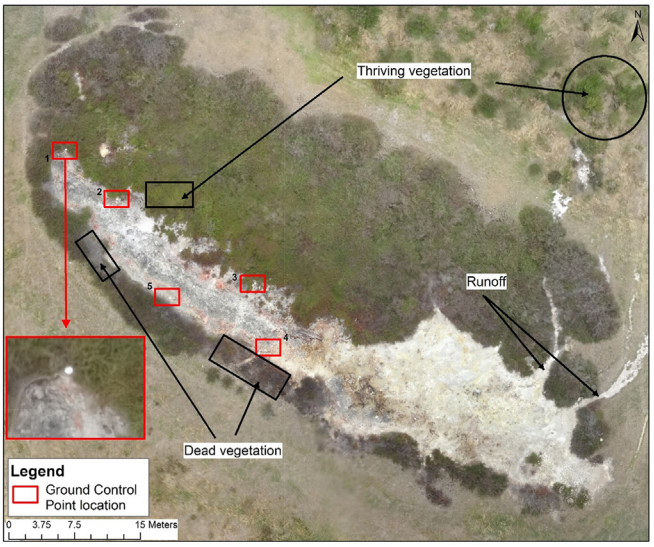

Fig. 3. Colour aerial image of the study area thermal feature and surroundings and showing the controls points. (For interpretation of the references to colour in this figure legend, the reader is referred to the web version of this article.)

3.1.4. Image processing

3.1.4.1. Colour aerial image processing. Over 1700 colour (RGB) images were captured. Each image was approximately 1.2 MB in size and 1920 × 1980 in dimension and was associated with an.xml file containing georeferencing data. Images were calibrated and orthomosaiced into one image of the entire study area using Pix4Dmapper (http://pix4d.com). At the time of the study, two supported UAV Image processing software packages dominated the market, Agisoft PhotoScan and Pix4Dmapper. Pix4Dmapper was chosen due to its comprehensive camera database which was always found to be updated, excellent technical support, good collection of documentation and more options for outputting data.

During the 2010 earthquake recovery in Haiti, Pix4UAV (previous name) was used by the International Organisation for Migration and United Nations Operational Satellite Application programme to produce the overview mosaic and elevation model for the topographical and hydrographical studies [112,94]. also demonstrated the capability of UVAs with Pix4UAV software to develop species specific vegetation maps in Australia.

The Pix4Dmapper applies computer visioning theory to compare conjugate points in overlapping images and determine their relative positions and orientations by bundle block adjustment [113]. Traditionally, about 20 key points per image are selected for matching but Pix4Dmapper uses up to 60,000 points. The software adjusts for focal length and lens distortion and the position and attitude of the camera. It also uses the relative views of neighbouring images to create a digital terrain model (DTM) with 3D coordinates for each image pixel [113]. The model is refined and positioned using independent georeferencing data and ground control points collected by GPS.

Pix4Dmapper can be run on a PC workstation but we chose to use Amazon cloud computing because of the number of images and amount of processing required. Amazon Cloud Computing (Amazon EC2) provides a range of computer capacities made available as virtual servers, Table 2 lists the specifications of the Cloud Computer used. Subsequent spatial and image analyses were processed in ArcGIS 10.2.

3.1.5. Thermal infrared aerial image processing

The FLIR Tau 320 unit captures grey scale video (.avi) without any georeferenced data. Still frames were subsampled from the video using tools developed in the 'Python' program language. The tool was set to capture a still image at a rate of 1 per second from the video to provide 9846 infrared, grey scale images. The tool can be run from within ArcGIS as a script, or from the command line by supplying the required input parameters at run time.

The infrared images were mosaicked and modelled in Pix4Dmapper by the cloud computer in a process similar to that used for the colour images except that camera specifications had to be manually calibrated and the resulting mosaic was not georeferenced. The

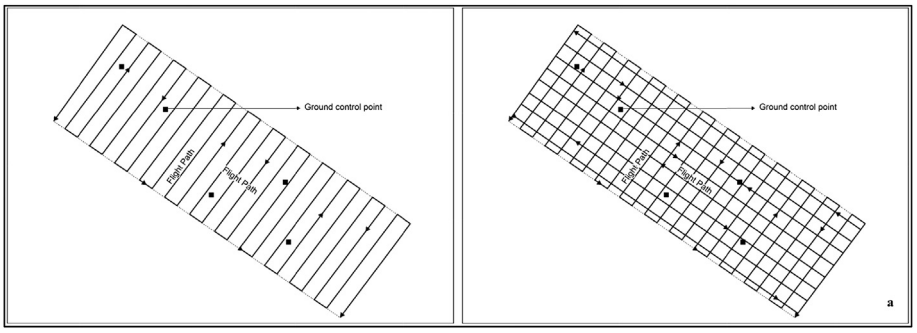

Fig. 2. Planned flight path for colour aerial image capture and the positions of control points. Fig. 2a: Planned flight path for thermal infrared video capture and the positions of control points.

infrared orthomosaic was georeferenced in ArcGIS 10.2 using the GPS coordinates of the ground control points and then re-projected into same coordinate system (Universal Transverse Mercator Zone 60S with World Geocentric System 1984 datum) as the colour mosaic.

4. Results

4.1. Colour aerial image

The colour orthorectified mosaic (Fig. 3) has a pixel size of 1.8 cm. Due to choosing the right time of the day for flying; no shadows in the imagery were detected, maintaining the integrity of the geothermal area. The mosaic displays the boundary of the geothermal surface manifestations clearly as bare ground with patches of white, grey and pink contours caused by the geothermal heat and the chemical discharge. The mosaic also shows the runoff channel caused during the last heavy rainfall. The vegetation surrounding the surface manifestations exhibit colours ranging from healthy green to brown and grey dead plants. The main purpose of the colour imagery was to provide the GCPs for georeferencing the TIR imagery. Without any issue the GCPs were identified and its coordinates (Table 3) were extracted.

4.2. Thermal infrared aerial image

The orthomosaic of the thermal infrared imagery is shown in Fig. 4. The orthorectified mosaic has a pixel size of 0.5 cm, significantly better resolution than in the colour mosaic. The colour scale is non-linear. It stretches subtle differences near inferred ambient temperatures and compresses inferred temperature differences at higher temperatures. A warm to hot thermal anomaly range was computed by normalizing the values of the orthorectified mosaic.

Numerous warm to hot thermal anomalies exist in the study area, and appear as hot bare ground. These features are associated with steam heated ground rather than discharging geothermal springs or streams. The inferred TIR image shows that inferred high temperatures (red colour, temperatures >90 °C) occur and dominate west side of the surface manifestation, whereas the warm areas (green to blue colours, temperatures < 50 °C) can be seen toward the southeast end. Emphasis was given to collecting images with a high overlap, the quality report from Pix4Dmapper application demonstrated the study area had more than five overlapping images per pixel from the overlap score.

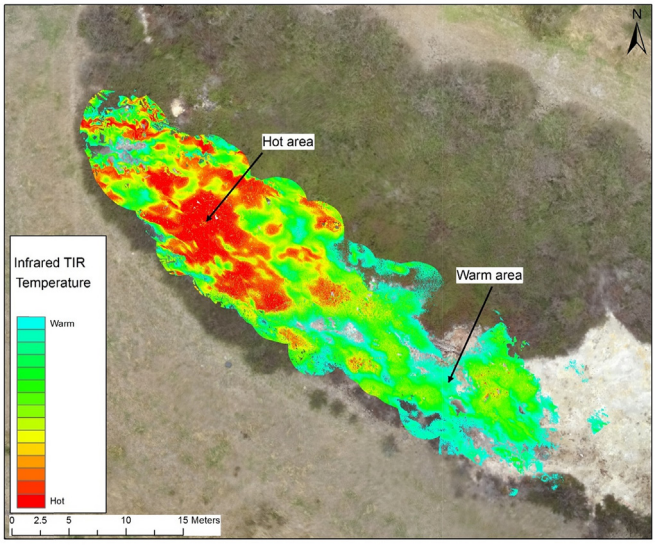

Fig. 4. Thermal infrared aerial image of the study area geothermal feature.

Table 3
Coordinates (NZTM) of the ground control points.

GCP	Easting	Northing
1	1870932.60450604	5713473.67771764
2	1870938.4141228	5713468.01442917
3	1870954.23200452	5713458.38145985
4	1870954.65745537	5713450.44394393
5	1870944.48473497	5713456.69870648

5. Discussion

In choosing a suitable UAV platform and sensors for this study, the specification was the main consideration. The Blade 350 QX quadcopter was purchased for under $1000 NZD, could be easily used in a difficult to access environment, was light weight and easy to transport over difficult terrain and had the functionality the carry out accurate aerial surveys and its affordability permits repeated surveys to detect change over time. Traditional aerial photography methods may be limited in this respect because of the high cost of obtaining repeated imagery.

The thermal infrared image of the study area was successfully captured, processed and projected. The 0.5 cm pixel size of thermal infrared mosaic is due to the quadcopter being able to fly at an elevation of 20 m to capture data. The colour orthorectified mosaic has a pixel size of 1.8 cm compared orthorectified mosaic to the one obtained from Land Information New Zealand (http://www.linz.govt.nz) which had a pixel size of 20 cm, imagery capture height being one of the major difference between the two sets of orthorectified mosaics. The resolution of the TIR image required depends on the area of study [63] and taking into account the size of the current study area, TIR imagery of high resolution was essential to display useful information [88]. were able to obtain a 29 cm resolution TIR imagery over an area of 2 km sq., using a manned aircraft flown at the average altitude of 600 m, the aim was to obtain TIR imagery with a much higher resolution than that.

There are cameras and sensors available for a variety of applications but it is important to acknowledge the payload limit of the UAV, and the risk of poor performance and loss of data quality [15]. The quadcopter used for this study successfully carried the 350 g FLIR tau 320 camera, but heavier loads would result in reduced flight times and increased thermal loads on the motors and controllers.

One limitation of this inexpensive quadcopter and transmitter was the inability to set waypoints and fly completely autonomously. UAV's offering waypoint navigation and autopilot options allow users to plan and program flight paths, heights and speeds [114]. This makes it easier to cover larger areas without losing battery time in manual manoeuvring. Without waypoint navigation, navigating a route to provide a suitable overlap between images has to be done visually, with the potential to leave gaps or sample unnecessarily. However by manually planning routes carefully along equally spaced transects, most of these problems were avoided in this study. However, this approach would be difficult and time consuming for larger survey areas.

Another limitation of using light small-sized UAVs is the lack of reliability to stay on a straight flight path or a fixed elevation, resulting in overlap variations and difference in rotation angles between adjacent images [79]. However, Pix4mapper with a standard aerial triangulation procedure is suited for orientation of images with irregular overlap acquired by UAVs [2]. Applications, like Pix4mapper, automate extraction of a consistent and redundant sets of tie points from images captured by UAV [58,76]. Pix4mapper

accomplish a fully automated project, requiring as input only camera calibration parameters and the images. Pix4mapper creates in an automatic way also the points cloud, the DSM and the orthophoto. The post processing matches points in overlapping image together creating a mosaic, the entire post processing is based on the values extracted from the images and the calibration of the camera [55] limiting external sources of errors.

While many efforts have been directed towards developing UAV control systems, communication and navigation [74] less attention has been paid to increasing the battery life for small UAV to maximise their flight time [96]. Current users overcome this challenge by carrying several charged batteries for replacement in the field. There are options [21,86] under investigation but not yet available in the market.

Being adamant about only flying in the appropriate weather condition paid off. No flight was attempted in wind spend more than 20 kn/hr, for both the colour and thermal infrared imagery capture it was very important to maintain the stability of the UAV and this would not have been possible in high winds. It was also noticed during the test flights that high wind speed and opposing wind direction consumed the batteries faster, shortening the flight time. For the dusk time flying, extra care had to be taken due to reduced visibility and the flights were suspended each time the wind picked up speed or changed course. The colour imagery showed minimal shadows, the existence of shadows makes it difficult to extract information [92]. TIR images were captured at dusk to reduce any solar radiation and the outputs did not show any irregularities that would suggest any solar interference.

Despite following the weather reports, the weather conditions are unpredictable and uncertain and can limit UAV operation. High wind conditions have a great impact on UAV performance [30] and was experienced during this study. Temperature, fog and rain can also impact UAV mission [87]. Information on weather is crucial for UAV mission planning and execution but the flight plan needs to be flexible to allow for weather circumstances. Considering weather condition is important not only because it could challenge the UAV flight settings and sensor payload, affecting the overall results but also compromise the safety of the pilot and the onlookers. Obtaining enough overlaps of the images were key since the raw images were to be processed using Pix4mapper, number of overlaps played a particular important role in the final mosaic quality. In this study we were able to obtain more than five overlaps per pixel which contributed to high resolution mosaic but took a considerable time to complete. The whole mosaicking procedure for colour imagery lasted for 10 h while the TIR mosaicking procedure lasting up to approximately 25 h, both processed using a cloud computer. The attempt on the desktop computer was still running after 4 day.

The FLIR Tau 320 was an appropriate thermal camera due to its small size (44.5 × 44.5 × 30.0 mm), light weight, low power consumption and cost. The 25 mm lens provided a flexible detection range suitable for use with a UAV without waypoint navigation and autopilot option. It can be a challenge maintaining a consistent flight height when flying manually. The detection range offered by the 25 mm lens allowed data to be reliably collected despite small variations in height.

It is a current industry practice to capture GCP locations using a differential GPS unit [49] but this study was limited by funds and the GCP locations were extracted from the geotagged colour imagery. Colour imagery capture of the study areas at the same time as TIR imagery also allowed for correlations between visible and thermal features. For example, the high temperature areas shown in the TIR imagery were seen as bare ground in the colour imagery.

The high interest in UAV's for civilian use [27] has prompted civil aviation authorities around the world to impose controls and regulations [27,35,56,105] and guidelines for appropriate use under certain conditions [60,82]. Where there is a need to operate outside regulations, it may be possible to request exemptions from local civil aviation authorities. One output of this research project is to provide recommendations on flying over geothermal areas to contribute to the development of appropriate guidelines and regulations.

Despite geothermal areas being protected from development, most are still within public access and it is vital to limit public access while flying over geothermal areas. It is important to have at least one other person involved apart from the flight operator to assist in keeping a watch for any ground or aerial hazards. Steam and hot water burns are potential risk of being near geothermal features due to which the UVA operator and all parties assisting should be in appropriate personal protective gear. Autonomous navigation systems make [15] reliable, systematic sampling designs relatively simple for even relatively inexperienced operators and improvements in these areas are matched by the advances in data processing and analysis techniques capable of handling thousands of images and variables [69].

To reduce the solar effects, TIR surveys are best flown at night [71]. Due to the restriction imposed by Civil Aviation Authority of New Zealand against flying UAVs after dark, TIR data was captured at dusk. The flying window was very short and multiple flights had to be planned and executed. With an increase in UAV applications for commercial, research and recreational use [31], regulations are necessary to protect the interest of all stakeholders. However specialist research such as carried out in this study may be dependent on certain conditions and these requirements needs to be taken into consideration. Aviation Authorities may need to look into different applications of UAV's and regulate accordingly to potentially allow for specialist use such as the capture of TIR data at night.

The future of UAV research within the geothermal sector is likely to explore applications not yet considered as improvements to platforms and the sensors continue to develop. The paramount benefit of using UAV is the reduction in costs [8]. The cost of an aeroplane, crew, fuel and camera involved in a traditional aerial survey [104] requires a significant budget compared to an UAV mission [48].

Furthermore, the increasing payloads of UAVs [52,89] and the variety [28] of small, light weight [1] sensors offering a high level of precision and data accuracy [39] at low altitudes make these tools increasingly valuable. With geothermal environment rapidly changing [11], UAV monitoring can provide a time and cost efficient solution for regular data capture to investigate changes in surface heat signatures, vegetation, geothermal surface features and geothermal energy production asset inspection. With the appropriate sensor [107], the possibilities are endless for both full motion video and still imagery capture. The implications of UVAs does not have to be limited for geothermal monitoring but can be replicated for mapping, feature detection and landform studies within any discipline.

6. Conclusion

In this article we demonstrated the use of UAVs for thermal infrared data capture in the geothermal environment and described an efficient method for data processing. FLIR Tau 320 sensor with a FLIR 25 mm lens attached on Blade 350 QX2 Quadcopter was used to capture thermal infrared image with a resolution of 0.5 cm, georeferencing it off the colour aerial imagery showing the five control points. Over other packages, Pix4Dmapper was used for image processing. The low cost and operational flexibility, along with the high spatial resolutions provided at high turnaround times, makes this platform suitable for this study as well as other number of applications. The study also highlights that while small UAVs do not provide a universal solution, they offer a cost-effective alternative to traditional manned aerial surveying.

The use of UAVs for environmental monitoring in the geothermal sector is still in its infancy despite potential

applications, low cost and operational flexibility. This is likely to change soon due to the tremendous leap forward in the availability and sophistication of UAV platforms and advances in processing software. Technological improvements such as platform stability, simple operational procedures, advanced payloads and operating range will undoubtedly play an important part in encouraging the diverse application of UAVs.

The current interest in UAV applications is provoking a new movement of emerging users keen to apply this technology in unconventional ways. It is important then that while maintaining safety, regulations allow for the development of this new research. UAV applications suit a variety of users, applications and budgets. Hence there is a need for users and aviation managers to work closely at this evolving stage in UAV technology to forge a safe and productive way forward.

Acknowledgement

The authors would like to thank Tauhara Middle 15 Trust for allowing the thermal infrared survey of their land. Robert Reeves of GNS Science is acknowledged for providing advice at the early stages of this project. Thanks to Terry Varhalamas, Patrick Englert, Tui Tuicena, and Fabian Sepulveda for assisting during UAV flying.

Appendix

Python Code for capturing stills from video using in ArcGIS 10.2 – "Process Videos tool".

```
import cv2
import os
import numpy
import arcpy

ws = arcpy.GetParameterAsText(0)
vidFormat = arcpy.GetParameterAsText(1)
imgFormat = arcpy.GetParameterAsText(2)
extPerSec - arcpy.GetParameterAsText(3)

def getVideoList(ws):
   lstVideos = os.listdir(ws)
   return lstVideos

def openVideo(ws,aFile):
   cam = cv2.VideoCapture(os.path.join(ws,aFile))
   fps = int(round(cam.get(5),0))
   return cam

def SaveFrame(cam,fName):
   cnt = 0
   run = 0
   fr = 30/extPerSec

   #run to end of file
   while run == 0:
      retval,camera_capture = get_image(cam)
      if retval == False:
         break
      theFile = os.path.join(fName,'img' + str(cnt/30) + imgFormat)
      #write one frame per second based on frame rate
      if cnt%fr == 0:
         print("Saving image...") + str(cnt/fr)
         cv2.imwrite(theFile, camera_capture)
         if camera_capture.size == None:
            break
      cnt += 1

def get_image(cam):
 retval, im = cam.read()
 return retval,im

def ProcessVideo(aVideo):
   fName = os.path.join(ws,aVideo[:-4])
   print fName
   os.mkdir(fName)
   cam = openVideo(ws,aVideo)
   SaveFrame(cam,fName)

lstVideos = getVideoList(ws)
for aVideo in lstVideos:
   if aVideo[-4:] == vidFormat:
      ProcessVideo(aVideo)
```

References

[1] A. Aguasca, R. Acevo-Herrera, A. Broquetas, J.J. Mallorqui, X. Fabregas, ARBRES: light-weight CW/FM SAR sensors for small UAVs, Sens. (Basel, Switz. 13 (3) (2013) 3204–3216.
[2] M. Ai, Q. Hu, J. Li, M. Wang, H. Yuan, S. Wang, A robust photogrammetric processing method of low-altitude UAV images, Remote Sens. 7 (3) (2015) 2302–2333.
[3] Y. Altshuler, V. Yanovski, I.A. Wagner, A.M. Bruckstein, Efficient cooperative search of smart targets using UAV swarms, Robotica 26 (4) (2008) 551–557.
[4] V.G. Ambrosia, S.S. Wegener, D.V. Sullivan, S.W. Buechel, S.E. Dunagan, J.A. Brass, J. Stoneburner, S.M. Schoenung, Demonstrating UAV-acquired real-time thermal data over fires, Photogramm. Eng. Remote Sens. 69 (4) (2003) 391–402.
[5] D.G. Barber, P.R. Richard, K.P. Hochheim, J. Orr, Calibration of aerial thermal infrared imagery for walrus population assessment, Arctic 44 (1991) 58–65.
[6] M. Bargh, Rethinking and re-shaping indigenous economies: maori geothermal energy enterprises, J. Enterp. Commun. 6 (3) (2012) 271–283.
[7] J.D. Barnes, J.L. Crosby, C.M. Jones, C.V.E. Wright, B.L.M. Hogan, Embryonic expression of Lim-1, the mouse homolog of xenopus XLim-1, suggests a role in lateral mesoderm differentiation and neurogenesis, Dev. Biol. 161 (1) (1994) 168–178.
[8] J. Berni, P.J. Zarco-Tejada, L. Suarez, E. Fereres, Thermal and narrowband multispectral remote sensing for vegetation monitoring from an unmanned aerial vehicle, Geosci. Remote Sens. IEEE Trans. 47 (3) (2009) 722–738.
[9] R. Bertani, Geothermal power generation in the world 2005–2010 update report, Geothermics 41 (2012) 1–29.
[10] H. Bibby, T. Caldwell, F. Davey, T. Webb, Geophysical evidence on the structure of the Taupo volcanic zone and its hydrothermal circulation, J. Volcanol. Geotherm. Res. 68 (1) (1995) 29–58.
[11] H.M. Bibby, A.W. Hurst, Tilt monitoring at wairakei geothermal field, Geothermics 19 (4) (1990) 385–396.
[12] T.L. Bott, T.D. Brock, Bacterial growth rates above 90 C in yellowstone hot springs, Science 164 (3886) (1969) 1411–1412.
[13] T.D. Brock, Life at high temperatures, Science 158 (3804) (1967) 1012–1019.
[14] T.D. Brock, G.K. Darland, Limits of microbial existence: temperature and pH, Science 169 (3952) (1970) 1316–1318.
[15] R. Brockers, M. Hummenberger, S. Weiss, L. Matthies, Towards autonomous navigation of miniature UAV, Comput. Vis. Pattern Recognit. Work. (CVPRW), 2014 IEEE Conf. (2014) 645–651.
[16] K.L. Brown, S.F. Simmons, Precious metals in high-temperature geothermal systems in New Zealand, Geothermics 32 (4) (2003) 619–625.
[17] B. Burns, Vegetation change along a geothermal stress gradient at the Te Kopia steamfield, J. R. Soc. N. Z. 27 (2) (1997) 279–293.
[18] D.W. Casbeer, D.B. Kingston, R.W. Beard, T.W. McLain, Cooperative forest fire surveillance using a team of small unmanned air vehicles, Int. J. Syst. Sci. 37 (6) (2006) 351–360.
[19] X. Chen, D.J. Campagna, Remote Sensing of Geology, The SAGE Handbook of Remote Sensing, 2009, 328.
[20] J.B. Corliss, J. Dymond, On the Galapagos Rift, Science 203 (1979) 16.
[21] L. Cwojdziński, M. Adamski, Power units and power supply systems in UAV, Aviation 18 (1) (2014) 1–8.
[22] B.M. Davis, The vegetation of the hot springs of Yellowstone park, Science 6 (135) (1897) 145–157.
[23] S. Daysh, M. Chrisp, Environmental planning and consenting for Wairakei: 1953–2008, Geothermics 38 (1) (2009) 192–199.
[24] D.J. Dickinson, Aerial infrared survey of Kawerau, Rotorua and Taupo urban areas – 1972, New Zealand, Dept. Sci. Indus. Res. 53 (1973). Geophys. Div. (Rept. No. 89).
[25] M.H. Dickson, M. Fanelli, Small geothermal resources: a review, Energy Sour. 16 (3) (1994) 349–376.
[26] R. DiPippo, Geothermal Power Plants: Principles. Applications and Case Studies, Wydawca Elsevier Advanced Technology, 2005.
[27] C. Drubin, UAV Market Worth $8.3 B by 2018, Microw. J. 56 (8) (2013) 37.
[28] P.J. Dziuban, A. Wojnar, A. Zolich, K. Cisek, W. Szumiński, Solid state sensors - practical implementation in unmanned aerial vehicles (UAVs), Procedia Eng. 47 (0) (2012) 1386–1389.
[29] H. Eisenbeiss, E.T.H. Zürich, UAV Photogrammetry, ETH, 2009.
[30] L. Evers, T. Dollevoet, A. Barros, H. Monsuur, Robust UAV mission planning, Ann. Oper. Res. 222 (1) (2014) 293–315.
[31] R.L. Finn, D. Wright, Unmanned aircraft systems: surveillance, ethics and privacy in civil applications, Comput. Law Secur. Rev. 28 (2) (2012) 184–194.
[32] I. FLIR, Tau Camera User's Manual, FLIR, Inc., Goleta, CA, 2010.
[33] I.B. Fridleifsson, R. Bertani, E. Huenges, J.W. Lund, A. Ragnarsson, L. Rybach, The possible role and contribution of geothermal energy to the mitigation of climate change, in: IPCC Scoping Meeting on Renewable Energy Sources, Proceedings, Citeseer, Luebeck, Germany, 2008.
[34] M. Funaki, N. Hirasawa, Outline of a small unmanned aerial vehicle (Ant-Plane) designed for Antarctic research, Polar Sci. 2 (2) (2008) 129–142.
[35] GCAA, GCAA to Issue UAVs Regulations, Emirates News Agency (WAM), Abu Dhabi, 2015.
[36] D.R. Given, Vegetation on heated soils at Karapiti, central North Island, New Zealand, and its relation to ground, N. Z. J Bot. 18 (1) (1980) 1–13.
[37] B. Glenn, Scout UAV gets new wrinkles, investment from Datron, Urgent Commun. (2011).
[38] G. Grindley, W.F. Harris, A. Steiner, The geology, structure and exploitation of the wairakei geothermal field, taupo, New Zealand: Palynology, Dep. Sci. IndusRes. (1965).
[39] R. Haarbrink, H. Eisenbeiss, Accurate DSM production from anned helicopter systems, Int. Arch. Photogramm. Remote Sens. Spat. Inf. Sci. 37 (2008) 1259–1264.
[40] M.C. Hanson, C. Oze, T.W. Horton, Identifying blind geothermal systems with soil CO_2 surveys, Appl. Geochem. 50 (0) (2014) 106–114.
[41] C. Haselwimmer, A. Prakash, Thermal Infrared Remote Sensing of Geothermal Systems. Thermal Infrared Remote Sensing, Springer, 2013, pp. 453–473.
[42] H.P. Heasler, C. Jaworowski, D. Foley, Geothermal systems and monitoring hydrothermal features, Geol. Monit. (2009) 105–140.
[43] W. Heise, H.M. Bibby, T.G. Caldwell, S.C. Bannister, Y. Ogawa, S. Takakura, T. Uchida, Melt distribution beneath a young continental rift: the Taupo Volcanic Zone, New Zealand, Geophys. Res. Lett. 34 (14) (2007).
[44] H.C. Helgeson, Geologic and thermodynamic characteristics of the Salton Sea geothermal system, Am. J. Sci. 266 (3) (1968) 129–166.
[45] M. Hochstein, Classification and Assessment of Geothermal Resources. Small Geothermal Resources: a Guide to Development and Utilization, UNITAR, New York, 1990, pp. 31–57.
[46] M.P. Hochstein, Crustal heat transfer in the Taupo volcanic zone (New Zealand): comparison with other volcanic arcs and explanatory heat source models, J. Volcanol. Geotherm. Res. 68 (1–3) (1995) 117–151.
[47] A. Hodgson, N. Kelly, D. Peel, Unmanned Aerial Vehicles (UAVs) for Surveying Marine Fauna: a Dugong Case Study, 2013.
[48] N. Hoffer, C. Coopmans, A. Jensen, Y. Chen, A survey and categorization of small low-cost unmanned aerial vehicle system identification, J. Intell. Robot. Syst. 74 (1–2) (2014) 129–145.
[49] P. Jayaprasad, B. Narender, S.K. Pathan, Ajai, Generation and validation of DEM using SAR interferometry and differential GPS supported by multi-spectral optical data, J. Indian Soc. Remote Sens. 36 (4) (2008) 313–322.
[50] A.G. Johnson, C.R. Glenn, W.C. Burnett, R.N. Peterson, P.G. Lucey, Aerial infrared imaging reveals large nutrient-rich groundwater inputs to the ocean, Geophys. Res. Lett. 35 (15) (2008) (n/a-n/a).
[51] K. Kaaniche, B. Champion, C. Pégard, P. Vasseur, A vision algorithm for dynamic detection of moving vehicles with a UAV, Robot. Autom. 2005. ICRA 2005. Proc. 2005 IEEE Int. Conf. IEEE (2005) 1878–1883.
[52] J. Kim, S. Lee, H. Ahn, D. Seo, S. Park, C. Choi, Feasibility of employing a smartphone as the payload in a photogrammetric UAV system, ISPRS J. Photogramm. Remote Sens. 79 (0) (2013) 1–18.
[53] W. Kissling, G. Weir, The spatial distribution of the geothermal fields in the Taupo Volcanic Zone, New Zealand, J. Volcanol. Geotherm. Res. 145 (1) (2005) 136–150.
[54] R. Krupp, T. Seward, The Rotokawa geothermal system, New Zealand; an active epithermal gold-depositing environment, Econ. Geol. 82 (5) (1987) 1109–1129.
[55] O. Küng, C. Strecha, A. Beyeler, J.-C. Zufferey, D. Floreano, P. Fua, F. Gervaix, The Accuracy of Automatic Photogrammetric Techniques on Ultra-light UAV Imagery, UAV-g 2011-Unmanned Aerial Vehicle in Geomatics, 2011.
[56] P. La Franchi, Civil UAV Regulations Edge Closer, Flight International, London, 2004. Reed Business Information UK. 165: 14.
[57] W. Lai, S. Kou, C. Poon, W. Tsang, C. Lai, Characterization of the deterioration of externally bonded CFRP-concrete composites using quantitative infrared thermography, Cem. Concr. Compos. 32 (9) (2010) 740–746.
[58] A.S. Laliberte, J.E. Herrick, A. Rango, C. Winters, Acquisition, orthorectification, and object-based classification of unmanned aerial vehicle (UAV) imagery for rangeland monitoring, Photogrammetric Eng. Remote Sens. 76 (6) (2010) 661–672.
[59] A.S. Laliberte, A. Rango, Image processing and classification procedures for analysis of sub-decimeter imagery acquired with an unmanned aircraft over arid rangelands, GISci. Remote Sens. 48 (1) (2011) 4–23.
[60] R.N. Laurence, FAA-type regulations will allow UAVs to grow, Aviat. Week & Space Technol. 155 (6) (2001) 70.
[61] K. Lee, Analysis of thermal infrared imagery of the Black Rock Desert geothermal area, Q. Colo. Sch. Mines 73 (3) (1978) (United States).
[62] S. Leroy, J. Anderson, J. Dykema, R. Goody, Testing climate models using thermal infrared spectra, J. Clim. 21 (9) (2008) 1863–1875.
[63] C.P. Lo, D.A. Quattrochi, J.C. Luvall, Application of high-resolution thermal infrared remote sensing and GIS to assess the urban heat island effect, Int. J. Remote Sens. 18 (2) (1997) 287–304.
[64] J.W. Lund, Geothermal energy focus: tapping the earth's natural heat, Refocus 7 (6) (2006) 48–51.
[65] D.W. Lynn, Monotemporal, multitemporal, and multidate thermal infrared data acquisition from satellites for soil and surface-material survey, Int. J. Remote Sens. 7 (2) (1986) 213–231.
[66] M. Mangiameli, G. Muscato, G. Mussumeci, C. Milazzo, A GIS application for UAV flight planning, Res. Educ. Dev. Unmanned Aer. Syst. 2 (1) (2013) 147–151.
[67] T.A. Mastor, N.A. Sulaiman, S. Juhari, A.M. Samad, An unmanned aerial imagery capturing system (UAiCs): a review of flight mission planning, Signal Process. Its Appl. (CSPA), 2014 IEEE 10th Int. Colloquium On. (2014) 129–133.
[68] A. McNabb, The Taupo-rotorua Hot-plate, 1992. Proc. 14th New Zealand

Geothermal Workshop.
[69] F.J. Mesas-Carrascosa, I.C. Rumbao, J.A.B. Berrocal, A.G.-F. Porras, Positional quality assessment of orthophotos obtained from sensors onboard multi-rotor UAV platforms, Sens. (Basel, Switz. 14 (12) (2014) 22394–22407.
[70] P. Molchanov, R.I.A. Harmanny, J.J.M. de Wit, K. Egiazarian, J. Astola, Classification of small UAVs and birds by micro-Doppler signatures, Int. J. Microw. Wirel. Technol. 6 (Special Issue 3–4) (2014) 435–444.
[71] M.A. Mongillo, Aerial thermal infrared mapping of the Waimangu-Waiotapu geothermal region, New Zealand, Geothermics 23 (5–6) (1994) 511–526.
[72] M.A. Mongillo, C.J. Bromley, A helicopter-borne video thermal infrared survey of the rotorua geothermal field, Geothermics 21 (1–2) (1992) 197–214.
[73] A. Ollero, L. Merino, Unmanned aerial vehicles as tools for forest-fire fighting, For. Ecol. Manag. 234 (1) (2006) 263.
[74] U. Ozdemir, Y. Aktas, A. Vuruskan, Y. Dereli, A. Tarhan, K. Demirbag, A. Erdem, G. Kalaycioglu, I. Ozkol, G. Inalhan, Design of a Commercial Hybrid VTOL UAV System, J. Intell. Robot. Syst. 74 (1–2) (2014) 371–393.
[75] M. Pace, Forecasting Ecological Responses to Global Change: the Need for Large-scale Comparative Studies, Biotic Interactions and Global Change. Sinauer Associates, 1991, pp. 356–363.
[76] M. Pierrot-Deseilligny, L. De Luca, F. Remondino, Automated image-based procedures for accurate artifacts 3D modeling and orthoimage generation, Geoinformatics FCE CTU 6 (2011) 291–299.
[77] P.J. Pinter Jr., J.L. Hatfield, J.S. Schepers, E.M. Barnes, M.S. Moran, C.S. Daughtry, D.R. Upchurch, Remote Sensing for Crop Management, 2003.
[78] M. Reiter, C. Shearer, C. Edwards, Geothermal anomalies along the Rio Grande rift in New Mexico, Geology 6 (2) (1978) 85–88.
[79] F. Remondino, L. Barazzetti, F. Nex, M. Scaioni, D. Sarazzi, UAV photogrammetry for mapping and 3d modeling–current status and future perspectives, Int. Arch. Photogramm. Remote Sens. Spatial Inf. Sci. 38 (1) (2011) C22.
[80] J. Renner, D. White, D. Williams, Hydrothermal convection systems, Assess. Geotherm. Resour. United States—1975 U. S. Geol. Surv. Circ. 726 (1975) 5–57.
[81] A.L. Reysenbach, H. Ehringer, K. Hershberger, Microbial diversity at 83 degrees C in Calcite Springs, Yellowstone National Park: another environment where the Aquificales and “Korarchaeota” coexist, Extremophiles 4 (1) (2000) 61–67.
[82] A. Roberts, A. Tayebi, A new position regulation strategy for VTOL UAVs using IMU and GPS measurements, Automatica 49 (2) (2013) 434–440.
[83] J.C. Ross, Evaluating CFRP-masonry Bond Using Thermal Imaging, University of South Florida, 2013, 1548796 M.S.C.E.
[84] L. Rybach, Geothermal systems, conductive heat flow, geothermal anomalies, Geotherm. Syst. Princ. Case Hist. (1981) 3–36.
[85] Sabins, K. Lulla, Remote sensing: principles and interpretation, Geocarto Int. 2 (1) (1987), 66–66.
[86] B. Saha, E. Koshimoto, C.C. Quach, E.F. Hogge, T.H. Strom, B.L. Hill, S.L. Vazquez, K. Goebel, Battery health management system for electric UAVs, Aerosp. Conf. 2011 IEEE (2011) 1–9.
[87] B. Sauter, Weather Impacts on the Aerostar Unmanned Aircraft System Based on Climatology over the US/Mexico Border, DTIC Document, 2007.
[88] A. Savelyev, R. Sugumaran, surface temperature mapping of the university of northern iowa campus using high resolution thermal infrared aerial imageries, Sens. (Basel, Switz. 8 (8) (2008) 5055–5068.
[89] M. Selinger, Aerosonde developing UAV with more payload room, Aerosp. Dly. Def. Rep. 214 (24) (2005) 1.
[90] S.F. Simmons, M. Keywood, B.J. Scott, R.F. Keam, Irreversible change of the Rotomahana-Waimangu hydrothermal system (New Zealand) as a consequence of a volcanic eruption, Geology 21 (7) (1993) 643–646.
[91] S. Soengkono, A magnetic model for deep plutonic bodies beneath the central Taupo Volcanic Zone, North Island, New Zealand, J. Volcanol. Geotherm. Res. 68 (1) (1995) 193–207.
[92] H.-G. Sohn, K.-H. Yun, Shadow-effect correction in aerial color imagery, Photogrammetric Eng. Remote Sens. 74 (5) (2008) 611–618.
[93] B. Stark, B. Smith, Y. Chen, Survey of thermal infrared remote sensing for Unmanned Aerial Systems, Unmanned Aircr. Syst. (ICUAS), 2014 Int. Conf. IEEE (2014) 1294–1299.
[94] C. Strecha, A. Fletcher, A. Lechner, P. Erskine, P. Fua, Developing species specific vegetation maps using multi-spectral hyperspatial imagery from unmanned aerial vehicles, ISPRS Ann. Photogramm. Remote Sens. Spat. Inf. Sci. I (3) (2012) 311–316.
[95] D. Sullivan, J. Fulton, J. Shaw, G. Bland, Evaluating the sensitivity of an unmanned thermal infrared aerial system to detect water stress in a cotton canopy, Trans. ASABE 50 (6) (2007) 1955–1962.
[96] K.O. Suzuki, P. Kemper Filho, J. Morrison, Automatic battery replacement system for UAVs: analysis and design, J. Intell. Robot. Syst. 65 (1–4) (2012) 563–586.
[97] J. Tashan, R. Al-Mahaidi, Investigation of the parameters that influence the accuracy of bond defect detection in CFRP bonded specimens using IR thermography, Compos. Struct. 94 (2) (2012) 519–531.
[98] I.A. Thain, B. Carey, Fifty years of geothermal power generation at Wairakei, Geothermics 38 (1) (2009) 48–63.
[99] B.P. Tice, Unmanned aerial vehicles: the force multiplier of the 1990s, Airpower J. (1991) 41–54.
[100] P. van Blyenburgh, UAVs: an overview, Air Space Eur. 1 (5–6) (1999) 43–47.
[101] S.M. van Manen, R. Reeves, An assessment of changes in Kunzea ericoides var. microflora and other hydrothermal vegetation at the Wairakei–Tauhara Geothermal Field, New Zealand, Environ. Manag. 50 (4) (2012) 766–786.
[102] S. Venturi, S. Di Francesco, F. Materazzi, P. Manciola, UAV and GIS Integrated Vegetation Analysis of Trasimeno Lake, 2014. Lakes: the mirrors of the earth: 217.
[103] A. VillasBoas, Sony POV Action Camera (HDR-AS100V) (PCmag.com), 2014.
[104] J. Visser, “Cost of aerial surveys.”, Photogrammetria 18 (0) (1961) 6–12.
[105] B. Vogel, South Africa claims 'considerable progress' in shaping UAV regulations, Jane's Airpt. Rev. 26 (9) (2014).
[106] A.C. Watts, V.G. Ambrosia, E.A. Hinkley, Unmanned aircraft systems in remote sensing and scientific research: classification and considerations of use, Remote Sens. 4 (6) (2012) 1671–1692.
[107] K. Whitehead, C.H. Hugenholtz, S. Myshak, O. Brown, A. LeClair, A. Tamminga, T.E. Barchyn, B. Moorman, B. Eaton, Remote sensing of the environment with small unmanned aircraft systems (UASs), part 2: scientific and commercial applications, J. Unmanned Veh. Syst. 02 (03) (2014) 86–102.
[108] N. Wilson, J. Webster-Brown, K. Brown, Controls on stibnite precipitation at two New Zealand geothermal power stations, Geothermics 36 (4) (2007) 330–347.
[109] C.P. Wood, Calderas and Geothermal Systems in the Taupo Volcanic Zone, New Zealand (proceedings of the World Geothermal Congress), 1995.
[110] R. Wooding, Large-scale Geothermal Field Parameters and Convection Theory, Applied Mathematics Division, DSIR, Wellington, New Zealand, 1976.
[111] S.S. Yeh, A failure of imagination: unmanned aerial vehicles and international security.”, Comp. Strategy 30 (3) (2011) 229–241.
[112] Z. Zhang, Native Vegetation Classification Using Remote Sensing Techniques: a Case Study of Dairy Flat Regrowth Bush by Using the Aut Unmanned Aerial Vehicle, Auckland University of Technology, 2014.
[113] B. Bollard-Breen, J. Brooks, M.L. Jones, J. Robertson, S. Betschart, O. Kung, S. Craig Cary, C. Lee, S. Pointing, Application of an unmanned aerial vehicle in spatial mapping of terrestrial biology and human disturbance in the McMurdo Dry Valleys, East Antarctica, Polar Biol. 38 (4) (2015) 573–578.
[114] X. Prats, E. Santamaria, L. Delgado, N. Trillo, E. Pastor, Enabling leg-based guidance on top of waypoint-based autopilots for UAS, Aerosp. Sci. Technol. 24 (1) (2013) 95–100.